Eur Biophys J (2008) 37:829–842
DOI 10.1007/s00249-008-0284-1

ORIGINAL PAPER

Differences between the channels, currents and mechanisms of conduction slowing/block and accommodative processes in simulated cases of focal demyelinating neuropathies

Diana I. Stephanova · Mariya S. Daskalova

Received: 15 October 2007 / Revised: 21 January 2008 / Accepted: 31 January 2008 / Published online: 20 February 2008

Abstract To clarify the differences between the mechanisms of conduction slowing/block and accommodative processes in focal demyelinating neuropathies, this computational study presents the kinetics of the ionic, transaxonal and transmyelin currents defining the intracellular and electrotonic potentials in different segments of human motor nerve fibres. The computations use our previous double cable model of the fibres. The simulated fibres have focal demyelination of internodes, paranodes or both together. The intracellular potentials are defined mainly by the Na^+ current, as the contribution of the K^+ fast and K^+ slow currents to the total nodal ionic current is negligible. The paranodal demyelinations cause an increase in the transaxonal current and a decrease in the transmyelin current at the paranodal segments. However, there is an inverse relationship between the transaxonal and transmyelin currents at the same segments in the cases of internodal demyelination. The internodal ionic channels beneath the myelin sheath do not contribute to the intracellular potentials, but they show a high sensitivity to long-lasting pulses. The slow components of the electrotonic potentials depend on the activation of the channel types in the nodal or internodal axolemma, whereas the fast components of the potentials are determined mainly by the passive cable responses. However, the current kinetics changes (defining the investigated electrotonic changes) are relatively weak. The study summarizes the results from these modelling investigations on the mechanisms underlying the conduction slowing/block and accommodative processes in focal demyelinating neuropathies such as Guillain–Barré syndrome and multifocal motor neuropathy.

Keywords Channels · Currents · Demyelinating neuropathies · Computational neuroscience

Abbreviations

IFD	Internodal focal demyelination
PFD	Paranodal focal demyelination
PIFD	Paranodal internodal focal demyelination
PISD	Paranodal internodal systematic demyelination

Introduction

A major function of the nerve fibre is to transmit information reliably from one site to another. If the axon of a myelinated fibre remains in continuity despite alterations or demyelinations, the fibre may retain its ability to conduct nervous impulses, but the axonal demyelination can lead to a spectrum of conduction abnormalities. Conduction slowing or conduction block is a characteristic feature described in demyelinating neuropathies, such as Charcot-Marie-Tooth disease type 1A (CMT1A), chronic inflammatory demyelinating polyneuropathy (CIDP) (Cappelen-Smith et al. 2001; Nodera et al. 2004; Sung et al. 2004), *n*-hexane neuropathy (Chang et al. 1998; Kuwabara et al. 1993), Guillain–Barré syndrome (GBS) and multifocal motor neuropathy (MMN) (Kaji 2003; Kuwabara et al. 2002; Priori et al. 2005). CIDP is one of several chronic demyelinating neuropathies that can occur with other systemic diseases (Barohn et al. 1989; Gorson et al. 2000; Katz et al. 2000). GBS is classified into acute inflammatory demyelinating polyneuropathy (AIDP) and acute motor axonal

D. I. Stephanova (✉) · M. S. Daskalova
Institute of Biophysics, Bulgarian Academy of Sciences,
Acad. G. Bontchev Str., Bl. 21, Sofia 1113, Bulgaria
e-mail: dsteph@shiva.bio.bas.bg

neuropathy (AMAN) by pathological and electrodiagnostic criteria (Choudhury and Arora 2001; Feasby et al. 1986; Griffin et al. 1995).

In our previous papers (Stephanova and Alexandrov 2006; Stephanova and Daskalova 2008; Stephanova et al. 2006a, b, 2007a, b) multiple membrane properties (such as intracellular, electrotonic and extracellular potentials as well as strength–duration time constants, rheobases and recovery cycles) of human demyelinated motor nerve fibres have been investigated by mathematical models. The demyelinations were focal occurring at the internode, paranode or both. The studies showed that the changes in the multiple membrane properties cited above for the investigated demyelinations [such as internodal focal demyelination (IFD) (Stephanova et al. 2006a, b), paranodal focal demyelination (PFD) (Stephanova and Alexandrov 2006; Stephanova and Daskalova 2008) and paranodal internodal focal demyelination (PIFD) (Stephanova et al. 2007b)] are so slight as to be essentially indistinguishable from normal values in the cases without conduction block. The studies confirm that the transition from conduction slowing to conduction block of the intracellular potentials leads to amplification of the degree of these membrane property changes, as the direction of the changes is maintained (Stephanova and Alexandrov 2006; Stephanova and Daskalova 2008). The results also show that the membrane abnormalities simulated in the focally demyelinated cases are in good accordance with the data from the patients with GBS and MMN (Kaji 2003; Kuwabara et al. 2002; Priori et al. 2005; Nodera and Kaji 2006).

Threshold electrotonus can be measured in these diseases. According to Bostock (1995) the threshold electrotonus is coined for the changes in threshold produced by long-lasting DC pulses, as the accommodative changes in threshold largely parallel the underlying electrotonic changes in membrane potential. Moreover, the mechanisms of the accommodative processes based on the kinetics of the currents defining electrotonic potentials have been investigated for systematic demyelinations [such as internodal systematic demyelination (ISD), paranodal systematic demyelination (PSD) and paranodal internodal systematic demyelination (PISD), in Stephanova et al. (2007a)] of human motor nerve fibres.

In the present study, we compare the mechanisms of conduction slowing/block and accommodative processes based on the intracellular and electrotonic potentials, respectively, of focally demyelinated human motor nerve fibres. An analysis of the kinetics of the ionic, transaxonal and transmyelin currents defining these potentials in different segments of the fibres is presented. To show the differences between the mechanisms of the accommodative processes in focal and systematic demyelinations, a part of the results concerning the current kinetics in the systematic demyelinations will be compared with those presented here.

Methods

The electrophysiology of human motor nerve fibres can be studied successfully using a double cable model of these fibres (Stephanova and Bostock 1995, 1996). Our model is a further development of the previous remarkably detailed model by Halter and Clark (1991) in which the separation of the axonal membrane, myelin sheath and the corresponding compartments was first reported in the literature. As the double cable model is thoroughly described and discussed in each of our papers cited above, we will mention here only that the normal fibre has $N = 150$ myelin lamellae. The model axon comprises 30 nodes of Ranvier and 29 internodes. Each internode is divided into two paranodal and five internodal segments. All calculations are carried out for fibres with an axon diameter of 12.5 μm. The lengths of node, paranode and nodal center to nodal center are 1.5, 200 and 1400 μm, respectively. The temperature is 37°C. The normal myelin thickness is 2.4 μm. The total internodal diameter is 17.5 μm. The entire normal myelin sheath is characterized with C_{my} (myelin capacitance) 1.5 pF and R_{my} (myelin resistance) 250 MΩ, and the R_{pn} (paranodal seal resistance) is 125 MΩ. The characteristic parameters defining the investigated demyelinations are given in Table 1. The conduction velocity of 58 m/s at 37°C for the 17.5 μm

Table 1 Membrane parameter values and conduction velocities characteristic for human motor nerve fibres in the normal and demyelinated cases, when the demyelinations are mild (IFD 70%; PFD 70%; PIFD 70%; PISD 70%) and severe (IFD 96%; PFD 96; PIFD 96%; PISD 82%)

	N	R_{my} [MΩ]	C_{my} [pF]	R_{pn} [MΩ]	v [m/s]
Normal	150	250.0	1.5	125.0	58
IFD 70%	*47*	*78.3*	*4.8*	125.0	40
PFD 70%	150	250.0	1.5	*39.0*	38
PIFD 70%	*47*	*78.3*	*4.8*	*39.0*	23
IFD 96%	*6*	*10.0*	*37.5*	125.0	0
PFD 96%	150	250.0	1.5	*5.0*	0
PIFD 96%	*6*	*10.0*	*37.5*	*5.0*	0
PISD 70%	*47*	*78.3*	*4.8*	*39.0*	25
PISD 82%	*27*	*45.0*	*8.3*	*22.5*	0

The membrane values showing the difference between the normal and each demyelinated case are italicized. The conduction velocities are calculated from the times of the intracellular potential maxima at the ninth and tenth nodes

N number of myelin lamellae, R_{my} myelin resistance, C_{my} myelin capacitance, R_{pn} paranodal seal resistance, v conduction velocity

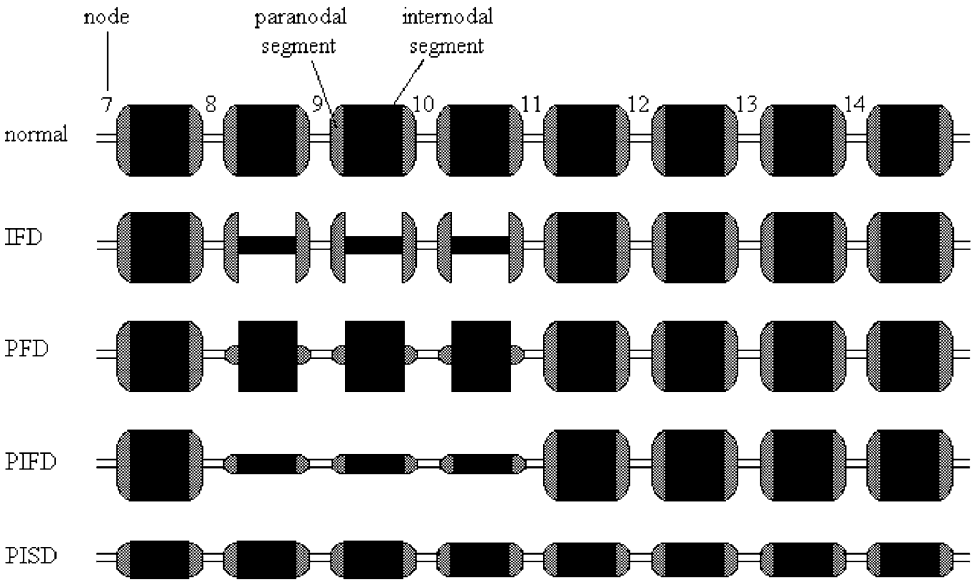

Fig. 1 Schematic diagram of human motor nerve fibres from the 7th to the 14th nodes in the normal, focally and systematically demyelinated cases. The reduction of the myelin lamellae (*IFD*) or of the paranodal seal resistance (*PFD*) or simultaneously both of them (*PIFD*) is restricted to only three (eighth, ninth and tenth) consecutive internodes for the focally demyelinated cases. The simultaneous reduction of the myelin lamellae and paranodal seal resistance is uniform along the fibre length in the PISD case

diameter human fibre is achieved, which corresponds qualitatively with experimental data at similar temperature (Huxley and Stämpfli 1949; Rasminsky 1973; Dioszeghy and Stålberg 1992). The channel types and maximum permeabilities ($cm^3/s \times 10^{-9}$) are as follows: node, Na (sodium) 9, K_f (fast potassium) 0.07, K_s (slow potassium) 0.26; internode, Na* (sodium) 80, K_f* (fast potassium) 27, K_s* (slow potassium) 2, IR* (inward rectifier) 0.008, L_k* (leak) 0.0064. The asterisk denotes an internodal quantity.

The investigated demyelinations are associated with a corresponding loosing or lifting of the myelin end bulbs and myelin lamellae away from the axolemma (Fig. 1). In the figure, the reduction of the myelin lamellae (IFD) or of the paranodal seal resistance (PFD) or simultaneously of the paranodal seal resistance and myelin lamellae (PIFD) is restricted to only three (eighth, ninth and tenth) consecutive internodes. The investigations are performed for 70 and 96% myelin reduction values, as it was done in our previous studies (Stephanova and Alexandrov 2006; Stephanova and Daskalova 2008). The first value is not sufficient to develop a conduction block of the intracellular potentials in the focally demyelinated cases and the demyelinations are regarded as mild. The second value leads to conduction block of the intracellular potentials in the investigated demyelinations. Such demyelinations are regarded as severe. The paranodal internodal systematic demyelination (PISD), as the most common case of various systematic demyelinations (Stephanova and Alexandrov 2006; Stephanova and Daskalova 2008), is used here, for a comparison with the focally demyelinated cases. (The simultaneous reduction of myelin lamellae and paranodal seal resistance in all internodes is termed paranodal internodal systematic demyelination.) The 70% reduction value is again not sufficient to develop a conduction block in the PISD. However, the conduction block is achieved when the myelin reduction value is 82%.

The intracellular potentials are simulated by adding a short (0.1 ms) rectangular current pulse to the center of the first node. This case of point application of current intra-axonally at the center of the node closely approximates the effects of point application of current extra-axonally at the node and realizes a point fibre polarization.

The electrotonic potentials are simulated by adding a 100 ms subthreshold current to the center of each internodal segment and the case of periodic kind of uniform fibre polarization is realized. The periodic kind of uniform polarization is first simulated in the human motor electrotonus model (Stephanova and Bostock 1996). The electrotonic potentials are calculated for depolarizing and hyperpolarizing currents, which correspond to 0.4 times the threshold for a 1 ms current pulse.

Results

Conduction slowing/block and accommodative processes based on the intracellular and electrotonic potentials, respectively

A comparison between the intracellular potentials is presented for the IFD, PFD, PIFD and normal cases without (Fig. 2a) and with (Fig. 2b) conduction block of human motor nerve fibres. The potentials are shown at each node, from the 7th to the 14th. For a better illustration, the normal case is repeated in the fourth column (Fig. 2a, b). The conduction proceeds into, through and beyond the demyelinated zone in the demyelinated cases (Fig. 2a). Although the rate of rise of the potential at the 8th, 9th and

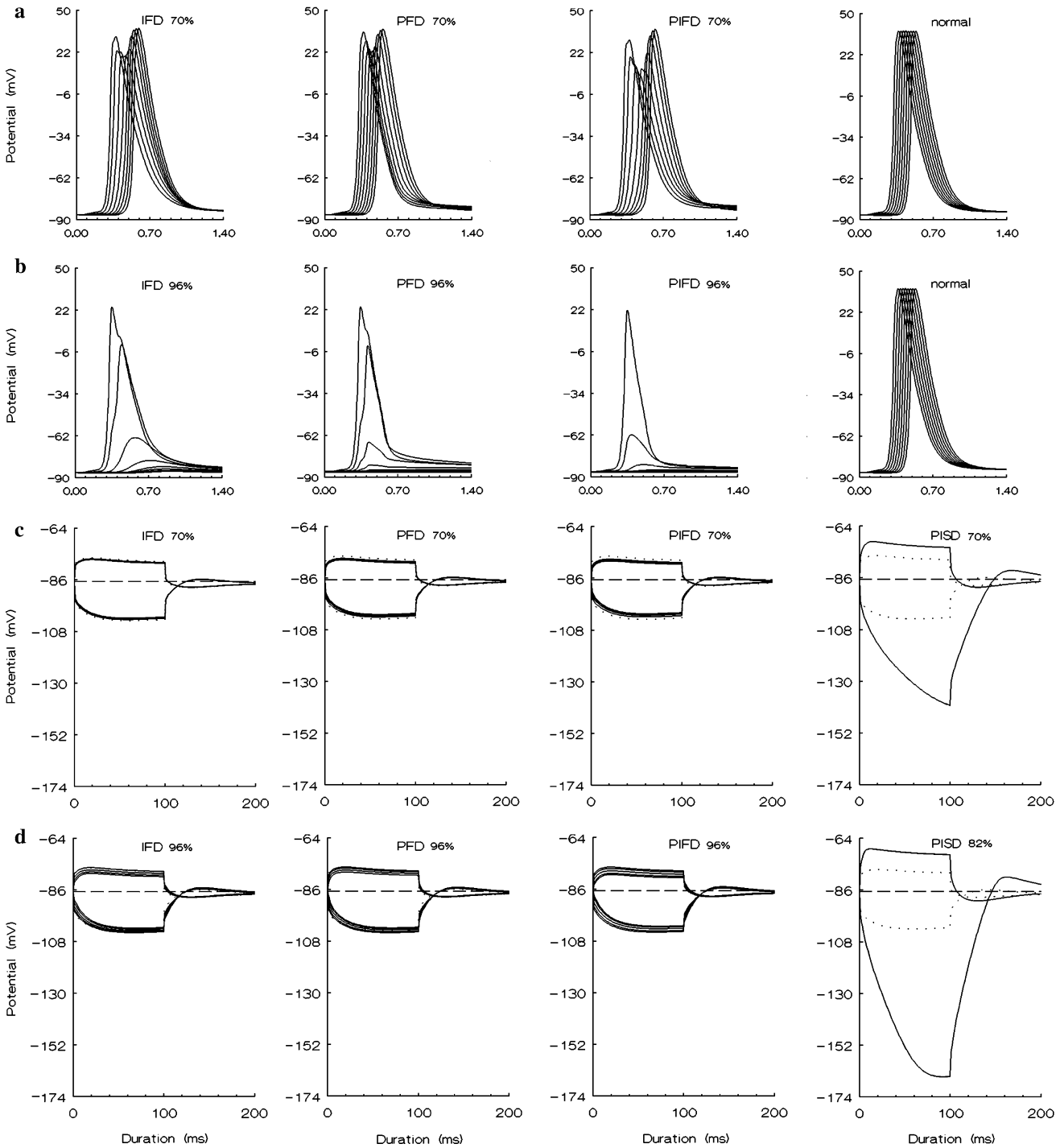

Fig. 2 Intracellular (**a, b**) and electrotonic (**c, d**) potentials in the mild (**a, c**) and severe (**b, d**) IFD, PFD, PIFD cases of human motor nerve fibres. These potentials are compared with those of the normal (the fourth column in **a, b**), mild and severe PISD cases (the forth column in **c** and **d**). The intracellular potentials are shown at each node, from the 7th to the 14th. The normal (*dotted lines*) and abnormal (*continued lines*) electrotonic potentials in response to 100 ms depolarizing and hyperpolarizing current pulses (±40% of threshold) are also presented at each node from the 7th to the 14th

10th nodes is gradually reduced, the potential recovers in the subsequent nodes. The potential amplitude achieves its normal value and the conduction occurs at its normal velocity in the regions distal to the demyelinated zone. In the cases of conduction block (Fig. 2b), the peak-to-peak amplitude of the potentials decreases until the potential dies out. The further reduction of the rate of rise of the potential at the nodes causes failure of the conduction.

A comparison of the electrotonic potentials is presented for the normal, IFD, PFD and PIFD cases, when the demyelinations are mild (Fig. 2c) and severe (Fig. 2d). To show the differences between the accommodative processes in the focally and systematically demyelinated cases, we have also added simulation of the PISD, which is mild or severe (Fig. 2c, d, in the fourth column). The temporal distributions of the potentials during and after 100 ms depolarizing and hyperpolarizing currents (±40% of threshold) are at each node, from the 7th to the 14th. For all focally demyelinated cases, the polarizing electrotonic potentials are similar, with a small drop to a minimum amplitude in the tenth node and with a small rise to a maximum amplitude in the 14th node. The transition from mild to severe demyelination leads to amplification of the degree of the potential changes, as the direction of these changes is maintained. In the mild and severe PISD cases each node behaves identically, and an overlap of the potentials at the nodes is obtained. The same is also valid for the normal case. When these cases are compared with the focal cases, the obtained differences are the greater increase in the depolarizing responses and the abnormally increase in the hyperpolarizing responses. The potentials are the most abnormal in the severe PISD case (Fig. 2d).

Mechanisms of the conduction slowing/block

The observed changes in the intracellular potentials are determined by the current kinetics (Fig. 3) of the fibres. The shown currents are at node 10 (a, b, c), adjacent distal paranode (d) and mid-internode between nodes 10 and 11 (e). To provide a better illustration: (1) the nodal ionic currents (I_{Na}, I_{Kf}, I_{Ks}, I_i) are presented in Fig. 3a; (2) the nodal transaxonal current (I_a, dotted line) and the nodal external membrane current (I_m) are presented in Fig. 3b, and (3) all these currents are presented in Fig. 3c. Using the model, we can also distinguish between membrane currents across the nodal or internodal axolemma (I_a, dotted line in Fig. 3b–e) and the external membrane current (I_m, in Fig. 3b–e), which are usually not the same, since current can flow longitudinally in the periaxonal space. (In the paranodal and internodal fibre segments, the external membrane current (I_m, in Fig. 3d, e) is equal to the transmyelin current). In the normal, IFD, PFD, PIFD cases, the nodal I_{Na} current (Fig. 3a, c) is activated rapidly by membrane depolarization and then inactivates. The intracellular potentials at the nodal segments are defined mainly by this I_{Na} current, as the contribution of the I_{Kf} and I_{Ks} currents to the total nodal ionic current (I_i) is negligible. However, the externally recorded nodal inward current (I_m, in Fig. 3b, c) is less than the current across the nodal axolemma (I_a), because of the short-circuiting through the paranodal seal resistance (R_{pn}). Compared with the IFD case, the externally recorded nodal inward current (I_m, negative phase) in the PFD case is lower. The decrease of the paranodal seal resistance also results in increased positive phase (reflecting the capacitive leakage current) of the external membrane current. Similarly, considerably more outward current flows across the paranodal axolemma (I_a, in Fig. 3d) than is apparent from the current flowing across the myelin (I_m). However, compared with the normal case, the externally recorded membrane current (I_m, in Fig. 3b, c) and the transmyelin currents (I_m, in Fig. 3d, e) in the IFD and PIFD cases are of greater magnitude. The kinetics of the currents in the PIFD case is consistent with the effect of reduced myelin lamellae, additionally increased by reduced paranodal seal resistance. As in the normal case, for all demyelinated cases, the internodal ionic currents beneath the myelin sheath (I^*_{Na}, I^*_{Kf}, I^*_{Ks}, I^*_{IR}, I^*_{Lk}) do not change significantly during the intracellular potential, either at the paranode and mid-internode, and appear as straight lines in Fig. 3d, e, respectively. The transaxonal and transmyelin currents are equal at the mid-internode (I_a and I_m, in Fig. 3e).

In the case of conduction block, the kinetics of the currents discussed above is zero at the node 10, adjacent distal paranode and mid-internode between nodes 10 and 11. Our unpublished data also show that the current kinetics of the focally demyelinated cases at the investigated segments, compared to the current kinetics at the same segments of the systematically demyelinated cases is very similar. However, in the focally demyelinated cases, the processes are realized earlier.

Mechanisms of the accommodative processes in the normal, IFD, PFD and PIFD cases

The observed changes in the electrotonic potentials to the subthreshold polarizing current pulses are also determined by the current kinetics (Figs. 4, 5, 6, 7) of the fibres. To provide a better comparison, the ionic and I_a, I_m currents are illustrated in different figures, however, they will be discussed simultaneously. In the normal and mildly demyelinated cases, the currents are again at node 10 (a), paranode next to node 10 (b) and mid-internode between nodes 10 and 11 (c), whereas, for the severely demyelinated cases, the currents at the same segments are given in (d), (e) and (f), respectively. For a better illustration: (1) the currents of the normal case given in (a), (b), (c) are repeated in (d), (e), (f), respectively; (2) the asterisk is omitted in Figs. 4b, c, e, f and 6b, c, e, f and (3) the zero straight lines in Fig. 6b, c, e, f indicate the internodal I_{Na} current.

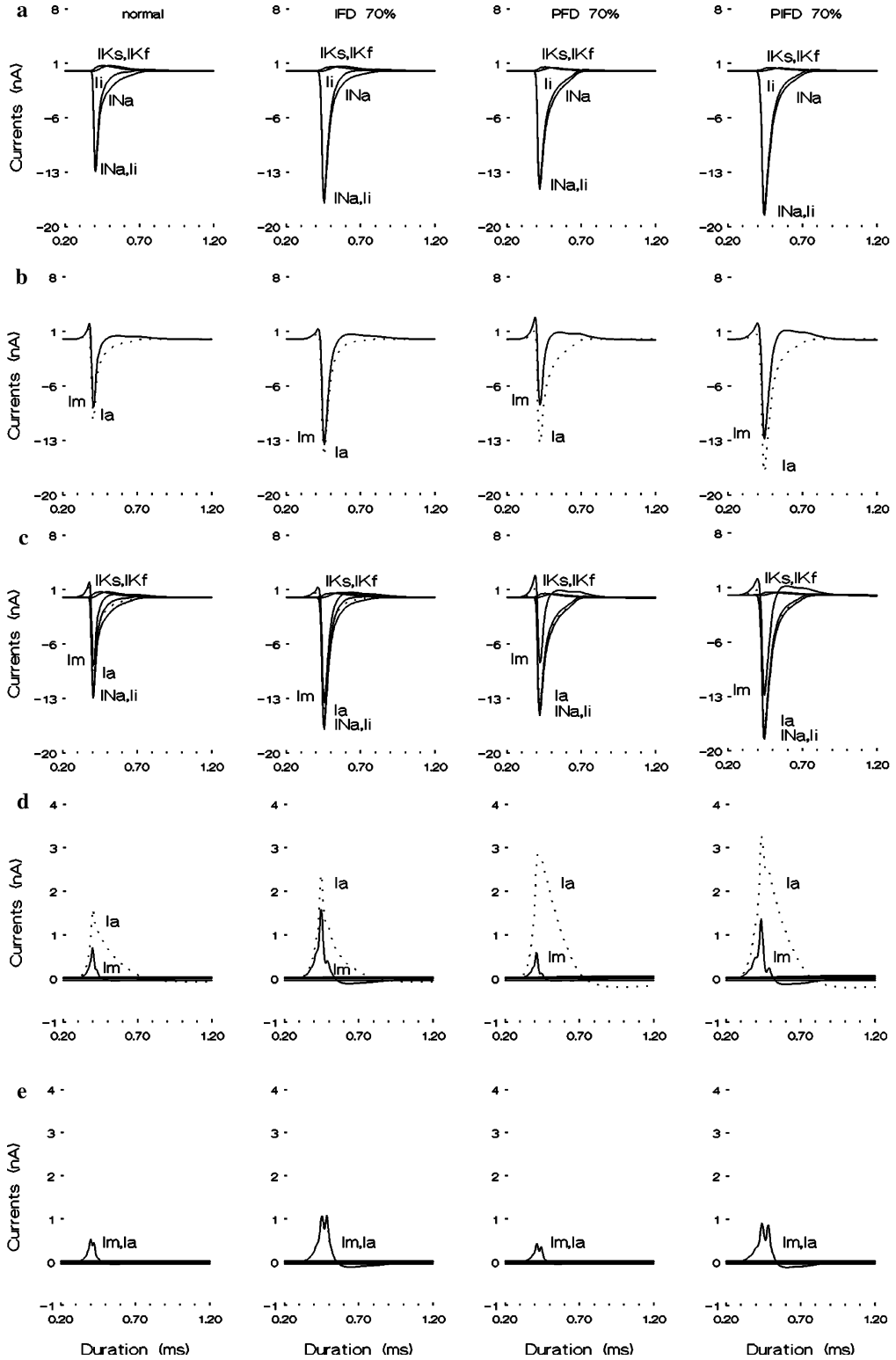

Fig. 3 Kinetics of the currents defining the intracellular potential in the normal, IFD, PFD and PIFD cases at node (**a–c**), adjacent distal paranode (**d**) and mid-internode between nodes 10 and 11 (**e**). The demyelinations (70%) are in the cases without conduction block of the intracellular potential. Currents: (**a**) nodal: I_{Na} (sodium), I_{Kf} (fast potassium), I_{Ks} (slow potassium), I_i (total ionic); (**b**) nodal: I_a (transaxonal), I_m (external membrane); (**c**) currents from (**a**) and (**b**) are given together; (**d, e**) internodal: I_a (transaxonal), I_m (transmyelin). The horizontal lines indicate the ionic currents: I^*_{Na} (sodium), I^*_{Kf} (fast potassium), I^*_{Ks} (slow potassium) I^*_{IR} (inward rectifier), I^*_{Lk} (leak). The *asterisk* denotes an internodal quantity

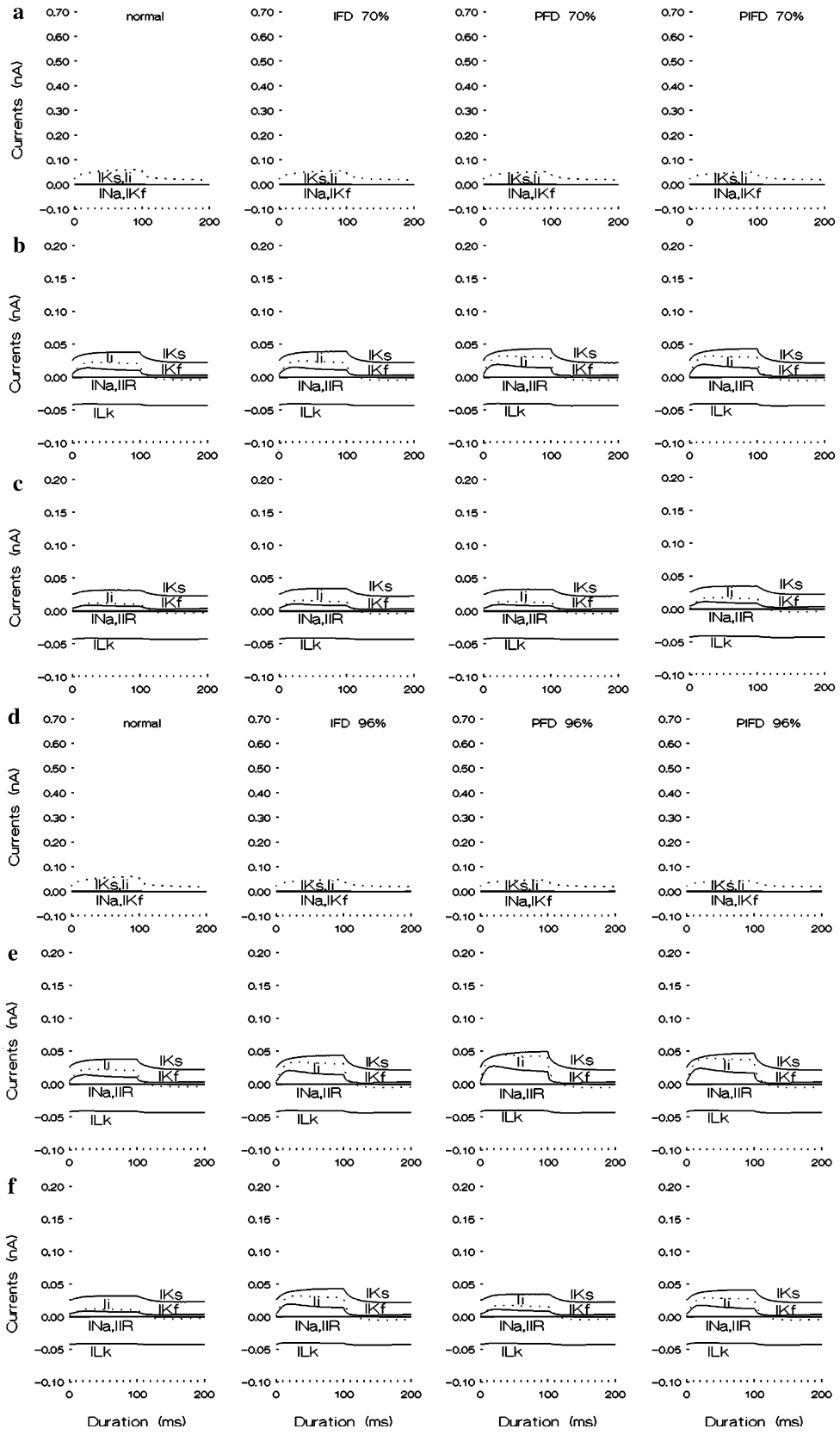

Fig. 4 During the subthreshold depolarizing current pulses, the kinetics of the ionic currents defining the electrotonic potential in the normal, IFD, PFD and PIFD cases is presented at node 10 (**a, d**), paranode next to node 10 (**b, e**) and mid-internode between nodes 10 and 11 (**c, f**) for the mild (70%) and severe (96%) demyelinations, respectively. Currents: I_{Na} (sodium), I_{Ks} (slow potassium), I_{Kf} (fast potassium), I_i (total ionic, *dotted lines*), I_{IR} (inward rectifier), I_{LK} (leakage)

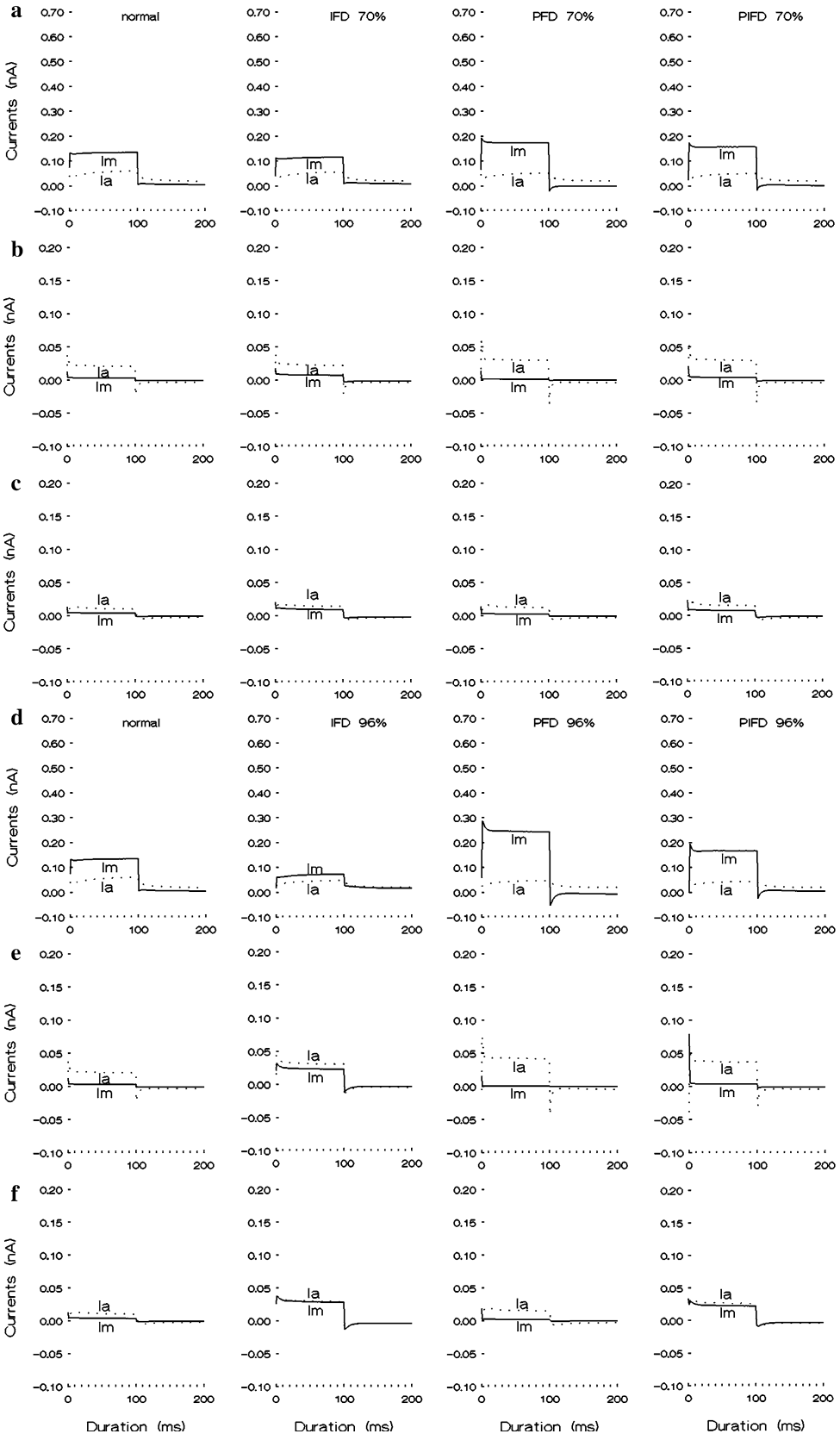

Fig. 5 During the subthreshold depolarizing current pulses, the kinetics of the transaxonal (I_a, *dotted lines*) and external membrane (I_m, *continued lines*) currents defining the electrotonic potential in the normal, IFD, PFD and PIFD cases is presented at node 10 (**a, d**), paranode next to node 10 (**b, e**) and mid-internode between nodes 10 and 11 (**c, f**) for the mild (70%) and severe (96%) demyelinations, respectively. In the paranodal and internodal segments, the external membrane current is equal to the transmyelin current

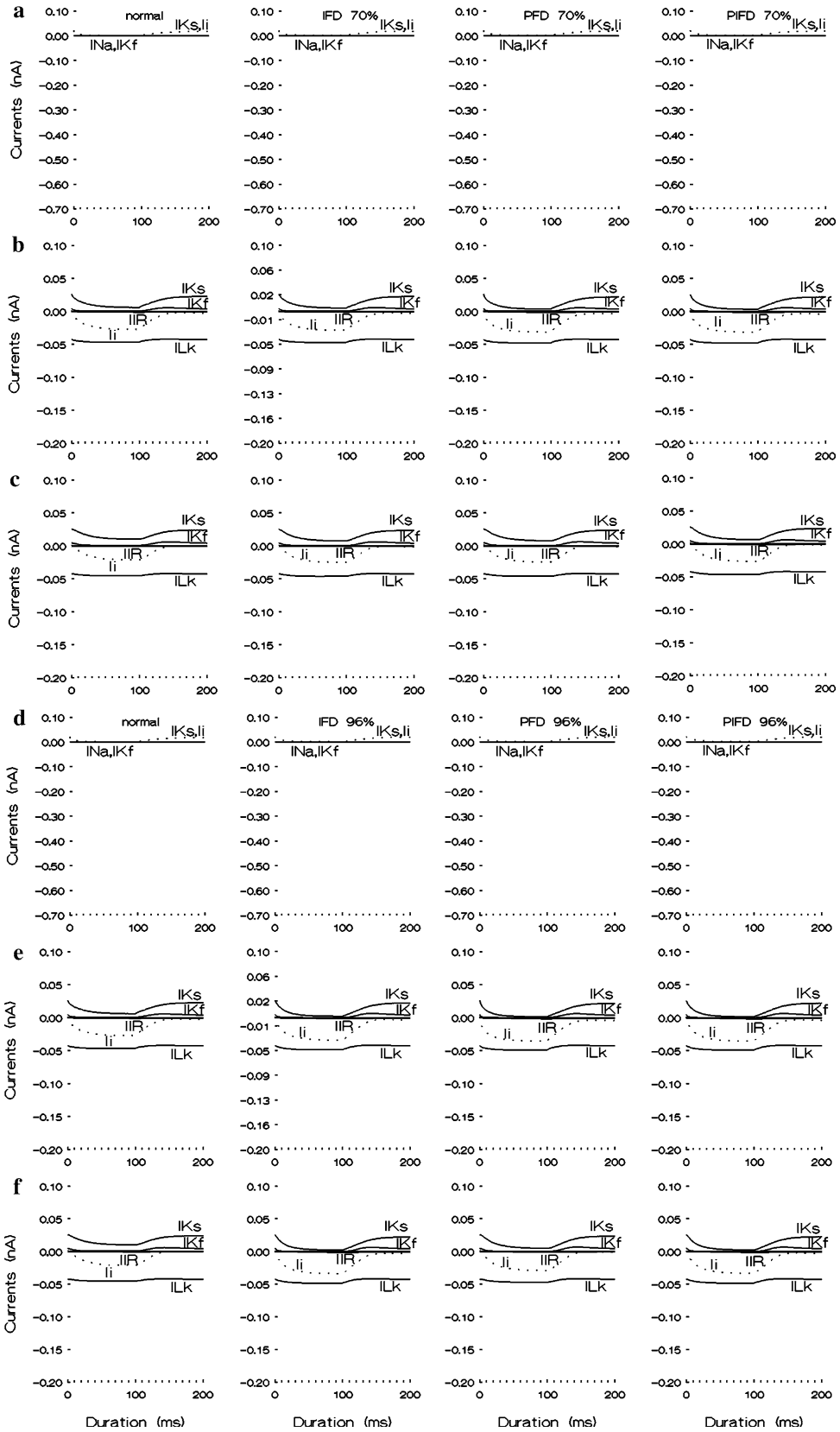

Fig. 6 During the subthreshold hyperpolarizing current pulses, the kinetics of the ionic currents defining the electrotonic potential in the normal, IFD, PFD and PIFD cases is presented at node 10 (**a, d**), paranode next to node 10 (**b, e**) and mid-internode between nodes 10 and 11 (**c, f**) for the mild (70%) and severe (96%) demyelinations, respectively. Currents: I_{Na} (sodium), I_{Ks} (slow potassium), I_{Kf} (fast potassium), I_i (total ionic, *dotted lines*), I_{IR} (inward rectifier), I_{LK} (leakage)

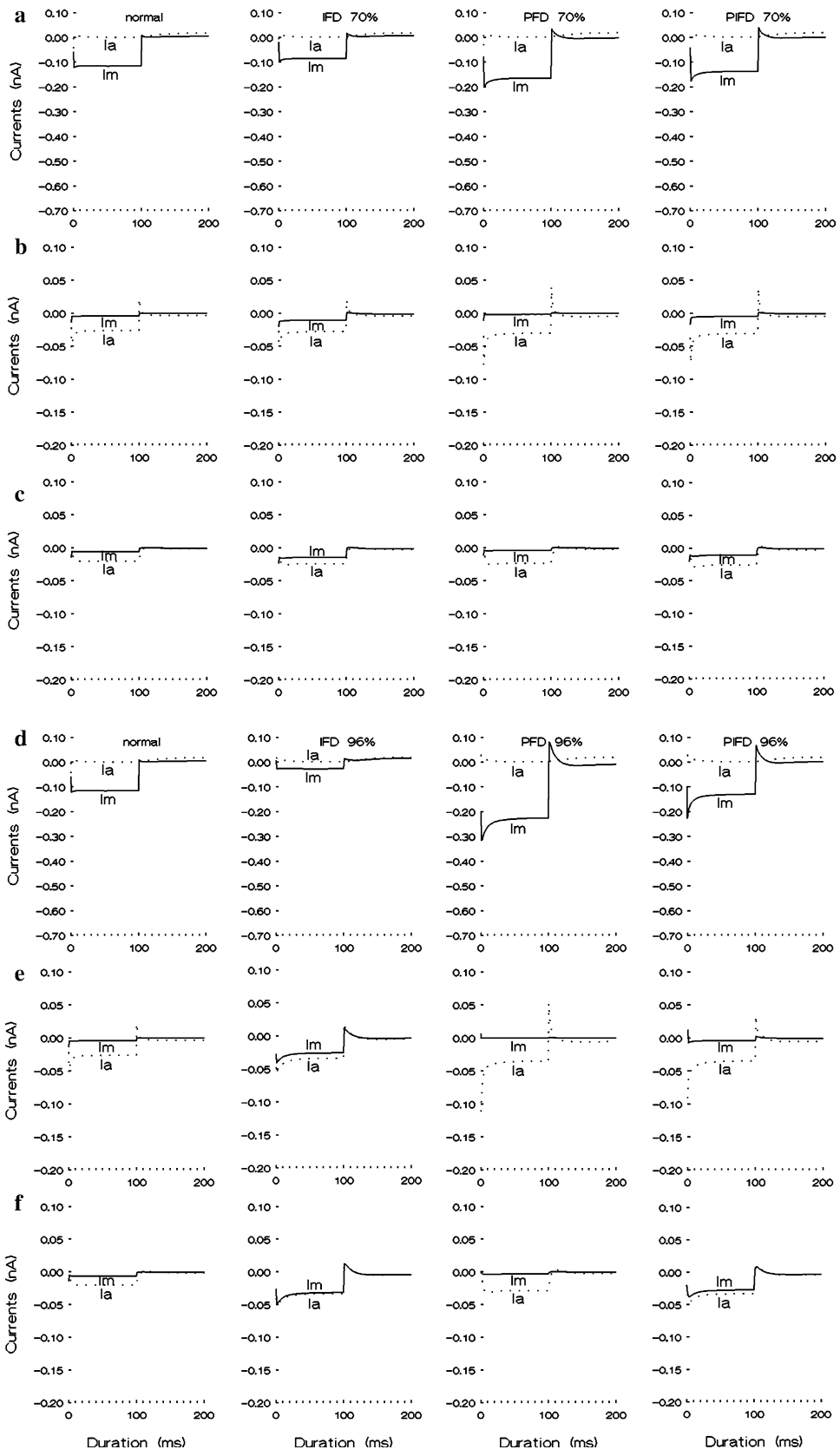

Fig. 7 During the subthreshold hyperpolarizing current pulses, the kinetics of the transaxonal (I_a, *dotted lines*) and external membrane (I_m, *continued lines*) currents defining the electrotonic potential in the normal, IFD, PFD and PIFD cases is presented at node 10 (**a, d**), paranode next to node 10 (**b, e**) and mid-internode between nodes 10 and 11 (**c, f**) for the mild (70%) and severe (96%) demyelinations, respectively. In the paranodal and internodal segments the external membrane current is equal to the transmyelin current

A. Current kinetics defining the depolarizing electrotonic potentials

The temporal distributions of the ionic (Fig. 4) and I_a, I_m (Fig. 5) currents are presented during the depolarizing current pulses. The results show that the contribution of nodal slow potassium current (I_{Ks}) to, both the total ionic current (I_i, dotted line in Fig. 4a, d) and the generation of the electrotonic potential in the normal and demyelinated cases, is obviously large. The other channels such as sodium (I_{Na}) and fast potassium (I_{Kf}) have minor contribution to the potential generation at the nodes. An overlap of the transaxonal (I_a, dotted line in Fig. 5a, d) and total nodal ionic current (I_i, dotted line in Fig. 4a, d) is obtained. Much of the externally recorded nodal current (I_m, continued line in Fig. 5a, d) does not flow across the axolemma, since I_a (dotted line) is much smaller, but passes longitudinally via the paranodal seal resistance to the periaxonal space. Conversely, considerably more currents flow across the paranodal and internodal axolemma (I_a, dotted line in Fig. 5b, c, e, f) than is apparent from the current flowing across the myelin sheath (I_m, continued line in Fig. 5b, c, e, f). For the same segments, the fast (I_{Kf}) and slow (I_{Ks}) potassium currents, resulting from activation of the ionic channels beneath the myelin sheath, dominate in the total ionic current (I_i, dotted line in Fig. 4b, c, e, f).

The decrease of the paranodal seal resistance causes an increase in both the external membrane current (I_m, PFD, in Fig. 5a, d) and the transaxonal current, as well as a decrease in the transmyelin current at the paranodal and internodal segments (I_a and I_m, PFD, in Fig. 5b, e), as the changes in the I_a are the biggest at the paranodal segments. However, there is an inverse relationship between the transaxonal (I_a) and transmyelin (I_m) currents at the paranodal and internodal segments in the IFD cases (I_a and I_m, IFD, in Fig. 5b, c, e, f). The current kinetics in the paranodal internodal demyelinations is consistent with the effect of the paranodal demyelination, additionally increased by the internodal demyelination (PIFD, in Figs. 4–5). The results also show that the changes in the ionic currents are so slight as to be essentially indistinguishable from normal values in the mild demyelinations (Fig. 4a–c). However, compared to the mild cases (Fig. 5 a–c), the I_a, I_m kinetics changes in the severe cases are bigger (Fig. 5d–f).

B. Current kinetics defining the hyperpolarizing electrotonic potentials

The contribution of the nodal ionic channels to the total ionic currents (I_i, dotted line) in the normal and abnormal cases (Fig. 6a, d) is negligible during the hyperpolarizing current pulses. Whereas at the paranodal and internodal segments, the activating slow potassium (I_{Ks}) and leak (L_k) channels dominate in the total ionic currents (Fig. 6b, c, e, f). Compared to the demyelinated cases during the depolarizing current pulses (Fig. 5), the kinetics of the transaxonal (I_a) and transmyelin (I_m) currents in the given different fibre segments is very similar (Fig. 7). However, these currents flow in the opposite direction during the hyperpolarizing current pulses.

Mechanisms of the accommodative processes in the mild and severe PISD cases

To show the differences between the mechanisms of the accommodative processes in the focal and systematic demyelinations (Fig. 2c, d), the current kinetics changes, defining the electrotonic potentials in the mild and severe PISD cases, are also presented (Fig. 8). They can be compared with those of the normal, mild and severe IFD, PFD and PIFD cases, which were shown and discussed above. The currents, defining the depolarizing electrotonic potentials, are again at node 10(a), paranode next to node 10(b) and mid-internode between nodes 10 and 11(c), whereas, for the hyperpolarizing potentials, the currents at the same segments are given in (d), (e) and (f), respectively. For a better comparison: (1) the ionic currents (first and second columns) and I_a, I_m currents (third and fourth columns) are illustrated in the same figure; (2) the asterisk (denoting the internodal ionic currents) is omitted in Fig. 8b, c, e, f, and (3) the zero straight lines in Fig. 8b, c, e, f indicate the internodal I_{Na} current. The results show that the mechanisms, defining the systematic electrotonic potentials, are the same as those described above for the focal electrotonic potentials. The main difference is that, the activating inward rectifier (IR) channels dominate in the total ionic currents at the paranodal and internodal segments of the systematically demyelinated cases. Moreover, the currents in the mild systematic demyelination (Fig. 8, first and third columns) abnormally increase when this demyelination is severe (Fig. 8, second and fourth columns). Compared to the mild and severe PISD cases, the current kinetics changes in the severe IFD, PFD and PIFD cases are relatively weak.

Discussion

In this study, the comparison between the conduction slowing/block and accommodative processes shows that their mechanisms are quite different in the normal and abnormal human motor nerve fibres. The gradually reduced amplitude, prolonged duration and slowed conduction velocity of the intracellular potentials passing through and beyond the demyelinated zone is an expected result in the

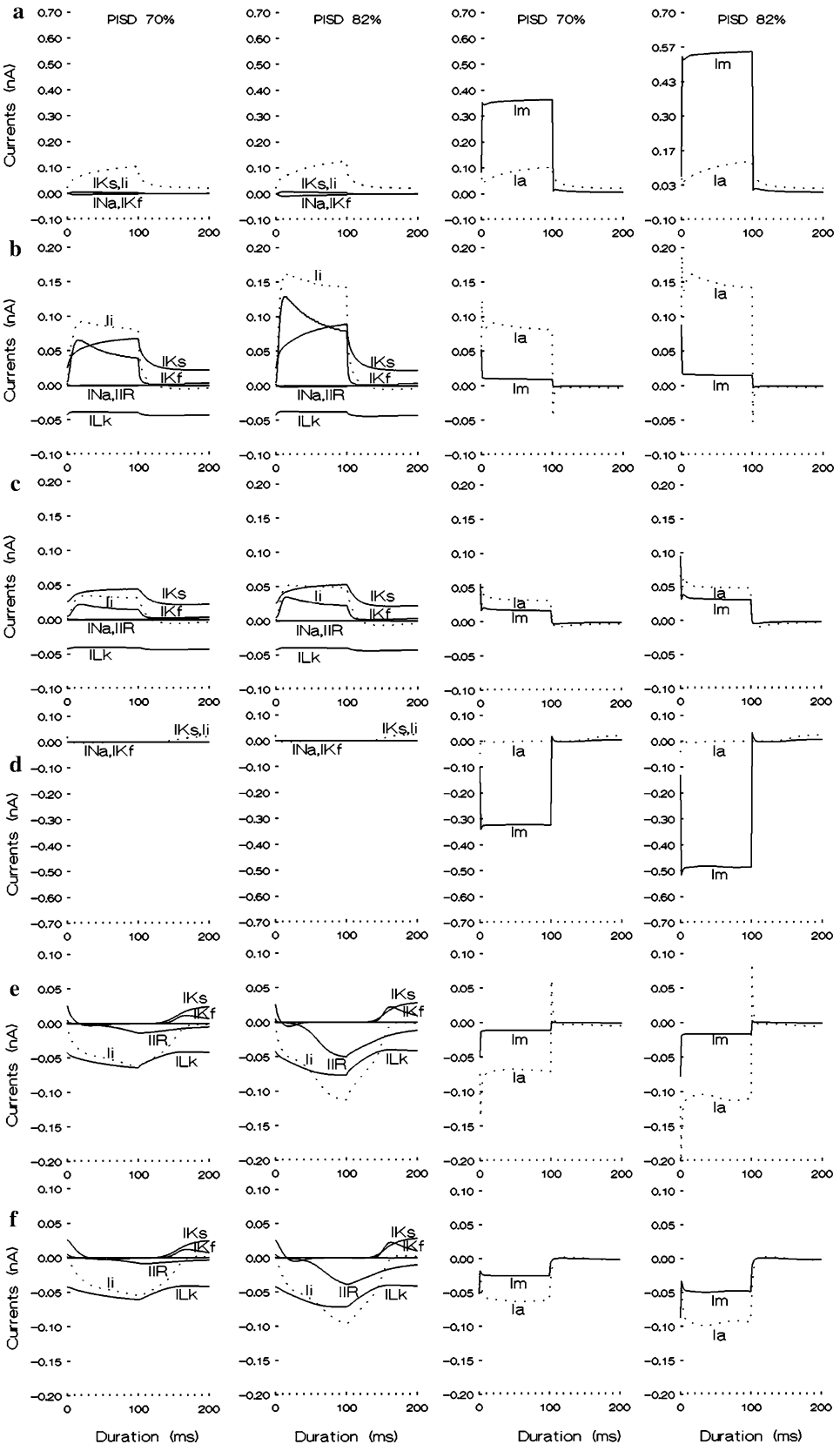

Fig. 8 The kinetics of the currents, defining the electrotonic potential in the mild (70%) and severe (82%) PISD cases is presented at node 10 (**a, d**), paranode next to node 10 (**b, e**) and mid-internode between nodes 10 and 11 (**c, f**) during the subthreshold depolarizing (**a, b, c**) and hyperpolarizing (**d, e, f**) current pulses. Currents: I_{Na} (sodium), I_{Ks} (slow potassium), I_{Kf} (fast potassium), I_i (total ionic, *dotted lines*), I_{IR} (inward rectifier), I_{LK} (leakage), I_a (transaxonal, *dotted lines*), and I_m (external membrane, *continued lines*)

focally demyelinated cases. The conduction block is a critical diagnostic feature in the GBS and MMN patients (Kaji 2003; Kuwabara et al. 2002; Priori et al. 2005; Nodera and Kaji 2006). Our results confirm that the classical "transient" Na^+ current contributes mainly to the intracellular potentials at the node. This current is activated rapidly by membrane depolarization and then inactivates. About 99% of the nodal Na^+ current behaves in this way. The remaining 1% "persistent" Na^+ current is activated at membrane potentials that are $\sim$10–20 mV more negative (Bostock and Rothwell 1997). This current is not simulated in the present study. However, according to the cited authors, the persistent nodal Na^+ current contributes mainly to the strength–duration time constants. The maximal amplitude, duration and afterpotential of the intracellular potential, calculated by us, match those of intracellular potential as measured in a node of Ranvier of single human myelinated nerve fibre (Schwarz et al. 1995). Our results also show that the internodal channels beneath the myelin sheath do not contribute to the intracellular potentials at the paranodal and internodal fibre segments. However, their contribution to the generation of the electrotonic potentials is significant.

The electrotonic potentials allow the accommodative responses to polarizing currents to be investigated in the normal and abnormal human motor nerve fibres. This study indicates a number of differences in the electrotonic potentials and their current kinetics between the normal and demyelinated cases when the latter are mild or severe. The described current kinetics of the electrotonic potentials shows that the slow (20–100 ms) components of the potentials are dependent on the activation of the channel types in the nodal or internodal axolemma, whereas the fast (0–20 ms) components of the potentials are determined mainly by the passive cable responses, i.e. by the capacitances and resistances of the corresponding different segments along the fibre. The present study also confirms that the kinetics of the currents, defining the electrotonic potentials is similar in the focally and systematically demyelinated cases. However, compared to the systematic cases, the current kinetics changes in the focal cases are relatively weak.

In conclusion, the conduction slowing/block and accommodative processes as characteristic features in demyelinating neuropathies are known to the neurophysiologists. However, the complex investigation of the current kinetics defining these processes in the focally demyelinated cases of human motor nerve fibres is first presented here. Our previous studies (Stephanova and Alexandrov 2006; Stephanova and Daskalova 2005a, b, 2008; Stephanova et al. 2005, 2006a, b, 2007a, b) show that the systematic demyelinations (ISD, PSD, PISD) are specific indicators for hereditary and chronic neuropathies (such as CMT1A and CIDP), whereas the focal demyelinations (IFD, PFD, PIFD) are specific indicators for acquired demyelinating neuropathies (such as Guillain–Barré syndrome and MMN). Consequently, this study provides important information about the electrogenesis of the demyelinating neuropathies.

References

Barohn RJ, Kissel JT, Warmolts JR, Mendell JR (1989) Chronic inflammatory demyelinating polyradiculoneuropathy; clinical characteristics, course and recommendations for diagnostic criteria. Arch Neurol 46:878–884

Bostock H (1995) Mechanisms of accommodation and adaptation in myelinated axons. In: Waxman SG, Kocses JD, Stys PK (eds) The axon. Oxford University Press, New Work, pp 311–327

Bostock H, Rothwell JC (1997) Latent addition in motor and sensory fibres of human peripheral nerve. J Physiol (Lond) 498:277–294

Cappelen-Smith C, Kuwabara S, Lin CS, Mogyoros I, Burke D (2001) Membrane properties in chronic inflammatory demyelinating polyneuropathy. Brain 124:2439–2447

Chang AP, England JD, Garcia CA, Summer AJ (1998) Focal conduction block in n-hexane polyneuropathy. Muscle Nerve 21:964–969

Choudhury D, Arora D (2001) Axonal Guillain–Barré syndrome: a critical review. Acta Neurol Scand 103:267–277

Dioszeghy P, Stålberg E (1992) Changes in motor and sensory nerve conduction parameters with temperature in normal and diseased nerve. Electroencephalogr Clin Neurophysiol 85:229–235

Feasby TE, Gilbert JJ, Brown WF, Bolton WF, Hahn AF, Koopman WF, Zochodne DW (1986) An acute axonal form of Guillain–Barré polyneuropathy. Brain 109:1115–1126

Gorson KC, Ropper AH, Adelman LS, Weinberg DH (2000) Influence of diabetes mellitus on chronic inflammatory demyelinating polyneuropathy. Muscle Nerve 23:37–48

Griffin JW, Li CY, Ho TW, Xue P, Macko C, Gao CY, Yang C, Tian M, Mishu B, Comblath DR (1995) Guillain–Barré syndrome in northern China. The spectrum of neuropathological changes in clinically defined cases. Brain 118:575–595

Halter J, Clark J (1991) A distributed-parameter model of the myelinated nerve fibre. J Theor Biol 148:345–382

Huxley AF, Stämpfli R (1949) Evidence for saltatory conduction in peripheral myelinated nerve fibres. J Physiol (Lond) 108:315–339

Kaji R (2003) Physiology of conduction block in multifocal motor neuropathy and other demyelinating neuropathies. Muscle Nerve 27:285–296

Katz JS, Saperstain DS, Gronseth G, Amato AA, Barohn RJ (2000) Distal acquired demyelinating symmetric neuropathy. Neurology 54:615–620

Kuwabara S, Nakajima M, Tsuboi Y, Hirayama K (1993) Multifocal conduction block in *n*-hexane neuropathy. Muscle Nerve 16:1416–1417

Kuwabara S, Ogawara K, Sung JY, Mori M, Kanai K, Hattori T, Yuki N, Lin CS, Burke D, Bostock H (2002) Differences in membrane properties of axonal and demyelinating Guillain–Barré syndromes. Ann Neurol 52:180–187

Nodera H, Bostock H, Kuwabara S, Sakamoto T, Asanuma K, Jia-Ying S, Ogawara K, Hattori N, Hirayama M, Sobue G, Kaji R (2004) Nerve excitability properties in Charcot-Marie-Tooth disease type A1. Brain 27:203–211

Nodera H, Kaji R (2006) Nerve excitability testing and its clinical application to neuromuscular diseases (invited review). Clin Neurophysiol 117:1902–1916

Priori A, Bossi B, Ardolino G, Ardolino G, Bertolasi L, Carpo M, Nobile-Orazio E, Barbieri S (2005) Pathophysiological heterogeneity of conduction blocks in multifocal motor neuropathy. Brain 128:1642–1648

Rasminsky M (1973) The effects of temperature on conduction in demyelinated single nerve fibres. Arch Neurol 28:287–292

Schwarz JR, Reid G, Bostock H (1995) Action potentials and membrane currents in the human node of Ranvier. Pflügers Arch 430:382–392

Stephanova DI, Alexandrov AS (2006) Simulated mild systematic and focal demyelinating neuropathies: membrane property abnormalities. J Integr Neurosci 5:595–623

Stephanova DI, Bostock H (1995) A distributed-parameter model of the myelinated human motor nerve fibre: temporal and spatial distributions of action potentials and ionic currents. Biol Cybern 73:275–280

Stephanova DI, Bostock H (1996) A distributed-parameter model of the myelinated human motor nerve fibre: temporal and spatial distributions of electrotonic potentials and ionic currents. Biol Cybern 74:543–547

Stephanova DI, Daskalova M (2005a) Differences in potentials and excitability properties in simulated cases of demyelinating neuropathies. Part II. Paranodal demyelination. Clin Neurophysiol 116:1159–1166

Stephanova DI, Daskalova M (2005b) Differences in potentials and excitability properties in simulated cases of demyelinating neuropathies. Part III. Paranodal internodal demyelination. Clin Neurophysiol 116:2334–2341

Stephanova D, Daskalova M (2008) Membrane property abnormalities in simulated cases of mild systematic and severe focal demyelinating neuropathies. Eur Biophys J 37:183–195

Stephanova DI, Daskalova M, Alexandrov AS (2005) Differences in potentials and excitability properties in simulated cases of demyelinating neuropathies. Part I. Clin Neurophysiol 116:1153–1158

Stephanova DI, Daskalova M, Alexandrov AS (2006a) Differences in membrane properties in simulated cases of demyelinating neuropathies. Internodal focal demyelinations without conduction block. J Biolog Phys 32:61–71

Stephanova DI, Daskalova M, Alexandrov AS (2006b) Differences in membrane properties in simulated cases of demyelinating neuropathies. Internodal focal demyelinations with conduction block. J Biol Phys 32:129–144

Stephanova DI, Daskalova M, Alexandrov AS (2007a) Channels, currents and mechanisms of accommodative processes in simulated cases of systematic demyelinating neuropathies. Brain Rese 1171:138–151

Stephanova DI, Alexandrov AS, Kossev A, Christova L (2007b) Simulating focal demyelinating neuropathies: membrane property abnormalities. Biol Cybern 96:195–208

Sung JY, Kuwabara S, Kaji R, Ogawara K, Mori M, Kanai K, Nodera H, Hattori T, Bostock H (2004) Threshold electrotonus in chronic inflammatory demyelinating polyneuropathy: correlation with clinical profiles. Muscle Nerve 29:28–37